Bifurcation Diagrams in the Landau–de Gennes Theory on Rectangles

Fang, Lidong (ldfang.sjtu@gmail.com)

School of Mathematical Sciences and Institute of Natural Sciences
Shanghai Jiao Tong University

joint work with Apala Majumdar (University of Bath)
and Lei Zhang (Shanghai Jiao Tong University)

The BOS (Bath Oxford Strathclyde) Network
22nd May, 2019

上海交通大學 SHANGHAI JIAO TONG UNIVERSITY

Liquid crystals

- Liquid crystals (LCs) are matter in a state between liquids and crystals. [Wikipedia: Liquid crystal].
- Liquid crystals may flow like a liquid, but oriented in a crystal-like way.
- Nematic phase: the rod-shaped molecules have long-range directional order and are free to flow.
- We study: Landau–de Gennes (LdG) theory and its bifurcation diagrams on rectangular domains.

Contents

SHANGHAI JIAO TONG UNIVERSITY

Landau–de Gennes Theory and Q–Tensor

- The Landau–de Gennes (LdG) theory [de Gennes and Prost, 1995] [Mottram and Newton, 2014] [Luo et al., 2012] [Henao et al., 2017] is a continuum theory for nematic liquid crystals that is defined in terms of a macroscopic order parameter – the LdG Q–tensor.
- The LdG Q–tensor is a symmetric and traceless tensor which can be viewed as a macroscopic measure of liquid crystal anisotropy or degree of orientational order. In 2D:

$$\mathbf{Q} = \begin{pmatrix} Q_{11} & Q_{12} \\ Q_{12} & -Q_{11} \end{pmatrix} := 2s\left(\mathbf{n} \otimes \mathbf{n} - \frac{\mathbf{I}_2}{2}\right) \tag{1}$$

- $\mathbf{n}(x)$ is the averaged director in some neighborhood B_x. Scalar order parameter $s(x) := \langle P_2(\cos(\theta - \theta_{\mathbf{n}}))\rangle_{B_x}$.
- $\mathbf{n} = (\cos\theta, \sin\theta)^T$, $Q_{11} = s\cos(2\theta)$, $Q_{12} = s\sin(2\theta)$.

Landau–de Gennes Theory and Q–Tensor

- The Landau–de Gennes (LdG) theory [de Gennes and Prost, 1995] [Mottram and Newton, 2014] [Luo et al., 2012] [Henao et al., 2017] is a continuum theory for nematic liquid crystals that is defined in terms of a macroscopic order parameter – the LdG Q–tensor.
- The LdG Q–tensor is a symmetric and traceless tensor which can be viewed as a macroscopic measure of liquid crystal anisotropy or degree of orientational order. In 2D:

$$\mathbf{Q} = \begin{pmatrix} Q_{11} & Q_{12} \\ Q_{12} & -Q_{11} \end{pmatrix} := 2s\left(\mathbf{n} \otimes \mathbf{n} - \frac{\mathbf{I}_2}{2}\right) \tag{1}$$

- $\mathbf{n}(x)$ is the averaged director in some neighborhood B_x. Scalar order parameter $s(x) := \langle P_2(\cos(\theta - \theta_{\mathbf{n}}))\rangle_{B_x}$.
- $\mathbf{n} = (\cos\theta, \sin\theta)^T$, $Q_{11} = s\cos(2\theta)$, $Q_{12} = s\sin(2\theta)$.

LdG Free Energy

- Simplest case (no external fields and surface effects),

$$I_{\mathrm{LdG}}(Q) := I_{\mathrm{el}}(Q) + I_{\mathrm{b}}(Q), \tag{2}$$

- Elastic energy, ($L_{\mathrm{el}} > 0$ be an elastic constant)

$$I_{\mathrm{el}}(Q) := \int_{\Omega} \left(\frac{L_{\mathrm{el}}}{2} \left| \nabla Q(x) \right|^2 \right) \mathrm{d}x. \tag{3}$$

- Bulk energy, (α, B, C be positive material constants)

$$I_{\mathrm{b}}(Q) := \int_{\Omega} \left(\frac{A}{2} \mathrm{Tr}\left(Q(x)^2\right) - \frac{B}{3} \mathrm{Tr}\left(Q(x)^3\right) + \frac{C}{4} \left(\mathrm{Tr}\left(Q(x)^2\right)\right)^2 \right) \mathrm{d}x, \tag{4}$$

where $A := \alpha(T - T^*)$, T is the temperature, T^* is a transition temperature above which the isotropic phase is stable.

Dimensionless LdG Model

- Scale from the original domain $\Omega := [0, aL] \times [0, bL]$ to the reference domain $\tilde{\Omega} := [0, a] \times [0, b]$.
- The total energy can be written in terms of dimensionless variables, in 2D [Luo et al., 2012],

$$I_{\mathrm{LdG}}(\mathbf{Q}) \propto \int_{\tilde{\Omega}} \left(|\nabla Q_{11}|^2 + |\nabla Q_{12}|^2 + \frac{1}{\epsilon^2} \left(Q_{11}^2 + Q_{12}^2 - 1 \right)^2 \right) \mathrm{d}x. \tag{5}$$

- We have only one parameter ϵ left. $\epsilon := L^{-1} \sqrt{L_{\mathrm{el}}/C}$.
- Euler–Lagrange equations,

$$\begin{cases} \Delta Q_{11} = \left(Q_{11}^2 + Q_{12}^2 - 1 \right) Q_{11}/\epsilon^2, \\ \Delta Q_{12} = \left(Q_{11}^2 + Q_{12}^2 - 1 \right) Q_{12}/\epsilon^2, \end{cases} . \tag{6}$$

Stable States in Confined Square Well

- 2D square confined square well ($80\mu\mathrm{m} \times 80\mu\mathrm{m} \times 2\mu\mathrm{m}$) with tangential boundary condition [Tsakonas et al., 2007].
- Small ϵ: diagonal solutions and rotated solutions [Tsakonas et al., 2007] [Luo et al., 2012] [Robinson et al., 2017].
- Large ϵ: well-order reconstruction solution (WORS, [Robinson et al., 2017]).

Stable States in Confined Square Well

- 2D square confined square well ($80\mu\mathrm{m} \times 80\mu\mathrm{m} \times 2\mu\mathrm{m}$) with tangential boundary condition [Tsakonas et al., 2007].
- Small ϵ: diagonal solutions and rotated solutions [Tsakonas et al., 2007] [Luo et al., 2012] [Robinson et al., 2017].
- Large ϵ: well-order reconstruction solution (WORS, [Robinson et al., 2017]).

LdG Solutions in Confined Square Well

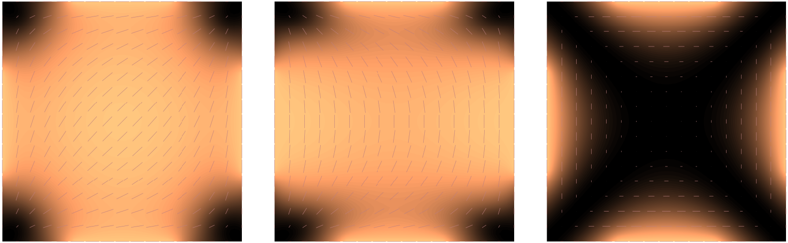

Figure: D1, R2 solutions at $\epsilon = 0.1$, WORS solution at $\epsilon = 0.4$. Darkest region: $s = 0$, lightest region: $s = 1$.

Boundary Conditions

- Tangential boundary condition for confined wells.
- The boundary condition is chosen as the one in the appendix of [Luo et al., 2012]. For $0 < d < 0.5$, we define the vector field g_d as,

$$g_d = \begin{cases} [T_{d/a}(x/a), 0], & y \in \{0, b\}, \\ [-T_{d/b}(y/b), 0], & x \in \{0, a\}, \end{cases} \tag{7}$$

where the trapezoidal function $T_d : [0,1] \to \mathbb{R}$ is given by,

$$T_d(t) = \begin{cases} t/d, & 0 \le t \le d, \\ 1, & d \le t \le 1-d, \\ (1-t)/d, & 1-d \le t \le 1. \end{cases} \tag{8}$$

- We use the strong anchoring Dirichlet boundary condition $(Q_{11}, Q_{12}) = g_{3\epsilon_0}$, $\epsilon_0 = 0.1$.

LdG Equation at Two Different ϵ Limits

- The micro–scale limit $\epsilon \to \infty$ ($L \to 0$) and the macro–scale limit $\epsilon \to 0$ ($L \to \infty$) for the LdG free energy,

$$\int_{\tilde{\Omega}} \left(|\nabla Q_{11}|^2 + |\nabla Q_{12}|^2 + \frac{1}{\epsilon^2} \left(Q_{11}^2 + Q_{12}^2 - 1 \right)^2 \right) \mathrm{d}x. \qquad (9)$$

- $\epsilon \to \infty$: The LdG equations become the separate Laplace equations $\Delta Q_{11} = \Delta Q_{12} = 0$.
- $\epsilon \to 0$: Minimizing the LdG free energy is equivalent to the constraint minimization problem,

$$\min_{Q_{11}^2 + Q_{12}^2 = 1} \int_{\tilde{\Omega}} \left(|\nabla Q_{11}|^2 + |\nabla Q_{12}|^2 \right) \mathrm{d}x. \qquad (10)$$

This is equivalent to the Oseen–Frank model,

$$\min_{n \in \mathbb{S}^1} \int_{\tilde{\Omega}} \left| \nabla n(x) \right|^2 \mathrm{d}x. \qquad (11)$$

LdG Equation at Two Different ϵ Limits

- The micro–scale limit $\epsilon \to \infty$ ($L \to 0$) and the macro–scale limit $\epsilon \to 0$ ($L \to \infty$) for the LdG free energy,

$$\int_{\tilde{\Omega}} \left(|\nabla Q_{11}|^2 + |\nabla Q_{12}|^2 + \frac{1}{\epsilon^2} \left(Q_{11}^2 + Q_{12}^2 - 1 \right)^2 \right) \mathrm{d}x. \tag{9}$$

- $\epsilon \to \infty$: The LdG equations become the separate Laplace equations $\Delta Q_{11} = \Delta Q_{12} = 0$.
- $\epsilon \to 0$: Minimizing the LdG free energy is equivalent to the constraint minimization problem,

$$\min_{Q_{11}^2 + Q_{12}^2 = 1} \int_{\tilde{\Omega}} \left(|\nabla Q_{11}|^2 + |\nabla Q_{12}|^2 \right) \mathrm{d}x. \tag{10}$$

  This is equivalent to the Oseen–Frank model,

$$\min_{n \in \mathbb{S}^1} \int_{\tilde{\Omega}} \left| \nabla n(x) \right|^2 \mathrm{d}x. \tag{11}$$

LdG Solution at Large ϵ Limits

- We can solve the Laplace equations by separation of variables on rectangles. Using the Dirichlet boundary conditions $(Q_{11}, Q_{12}) = g_{3\epsilon_0}$, we have,

$$
\begin{aligned}
&Q_{11}(x,y) \\
&= \sum_{k \text{ odd}} \frac{4\sin(k\pi d/a)}{k^2\pi^2 d/a} \sin\left(\frac{k\pi x}{a}\right) \frac{\sinh(k\pi(b-y)/a) + \sinh(k\pi y/a)}{\sinh(k\pi b/a)} \\
&\quad - \sum_{k \text{ odd}} \frac{4\sin(k\pi d/b)}{k^2\pi^2 d/b} \sin\left(\frac{k\pi y}{b}\right) \frac{\sinh(k\pi(a-x)/b) + \sinh(k\pi x/b)}{\sinh(k\pi a/b)}
\end{aligned} \tag{12}
$$

$$
Q_{12}(x,y) \equiv 0. \tag{13}
$$

LdG Solutions at Large ϵ

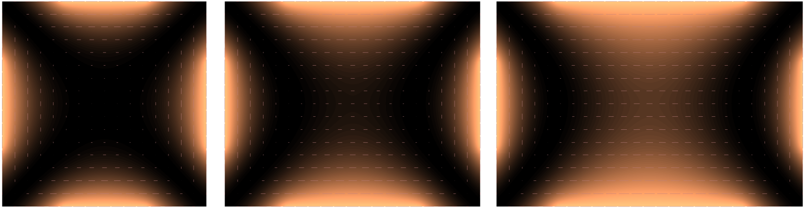

Figure: WORS and sBD2 solutions at $\epsilon = 100$. $a = 1, 1.25, 1.5$. Darkest region: $s = 0$, lightest region: $s = 1$.

Convergence at Large ϵ Limits

- $\Omega \subset \mathbb{R}^2$, smooth, bounded and simply connected.
- In the Landau–de Genes model, we write $u = (Q_{11}, Q_{12})^T$.

$$-\Delta u_\epsilon = \frac{1}{\epsilon^2} u_\epsilon \left(1 - |u_\epsilon|^2\right) \text{ in } \Omega, \quad u_\epsilon = g \text{ in } \partial\Omega, \tag{14}$$

where $g \in C^\infty\left(\partial\Omega; \mathbb{R}^2\right)$, $\left\| g|_{\partial\Omega} \right\|_{\ell^2} \leq 1$, $u_\epsilon \in H^1\left(\Omega; \mathbb{R}^2\right)$.

- u_ϵ is analytic [Majumdar and Zarnescu, 2010].
- $1 - |u_\epsilon|^2 \geq 0$ in Ω [Bethuel et al., 1993].
- The limit PDE is,

$$-\Delta u_\infty = 0 \text{ in } \Omega, \quad u_\infty = g \text{ in } \partial\Omega \tag{15}$$

where $u_\infty \in C^\infty\left(\Omega; \mathbb{R}^2\right)$.

- Convergence:

$$\forall i = 1, 2, \quad \left((u_\epsilon)_i - (u_\infty)_i\right) \sim \mathcal{O}\left(\epsilon^{-2}\right). \tag{16}$$

Numerical Convergence of sBD2 to Limit Solution

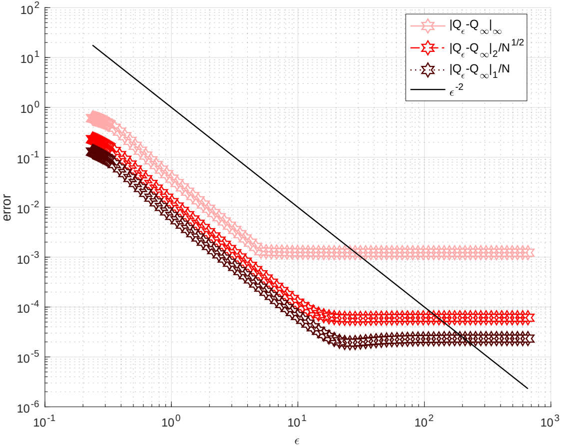

Figure: Domain size 1.25×1, mesh spacing $h = 1/64$.

Phase Transition between sD1 and sBD2

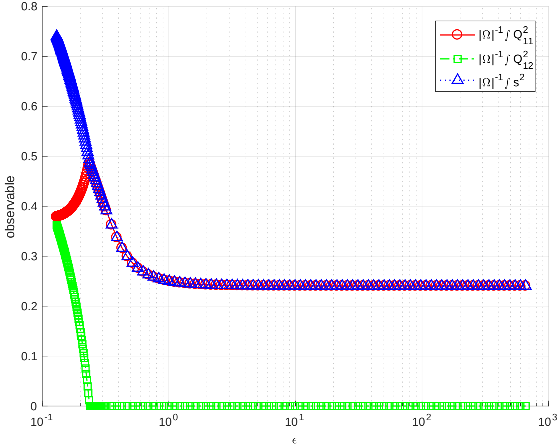

Figure: Domain size 1.25×1, mesh spacing $h = 1/64$.

Solution at Small ϵ Limits

- At small ϵ limit, we can solve $\theta : \Omega \to \mathbb{R}$,

$$\Delta\theta(x) = 0, \quad x \in \Omega. \tag{17}$$

  where θ is the angle of director n.
- We list different classes of solutions [Luo et al., 2012] using d_i, $i = 1, 2, 3, 4$ for the boundary conditions on $y = 0$, $x = a$, $y = b$, $x = 0$ respectively.

class	shape	d_1	d_2	d_3	d_4
D1	$/$	0	$+\pi/2$	0	$+\pi/2$
D2	$\backslash$	0	$-\pi/2$	0	$-\pi/2$
R1	$\subset$	0	$-\pi/2$	$-\pi$	$-\pi/2$
R2	$\supset$	0	$+\pi/2$	$+\pi$	$+\pi/2$
R3	$\cap$	0	$-\pi/2$	0	$+\pi/2$
R4	$\cup$	0	$+\pi/2$	0	$-\pi/2$

Table: Boundary Conditions of θ

上海交通大學 SHANGHAI JIAO TONG UNIVERSITY

Solution at Small ϵ Limits

- Again, using separation of variables, the solutions are,

$$\theta_{D1}(x,y) = \frac{\pi}{2}\left(f(y, a-x; b, a) + f(y, x; b, a)\right). \tag{18}$$

$$\theta_{R3}(x,y) = \frac{\pi}{2}\left(-f(y, a-x; b, a) + f(y, x; b, a)\right), \tag{19}$$

where,

$$f(x, y; a, b) = \sum_{k\ \text{odd}} \frac{4}{k\pi} \sin\frac{k\pi x}{a} \frac{\sinh\left(k\pi(b-y)/a\right)}{\sinh(k\pi b/a)}. \tag{20}$$

LdG Solutions at Small ϵ

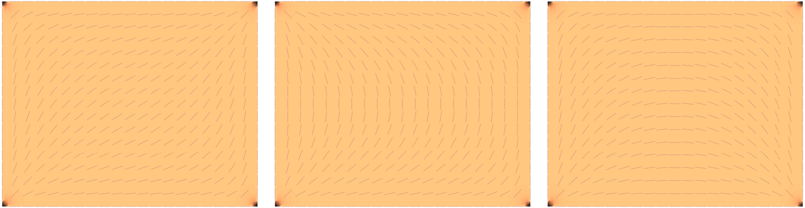

Figure: D1, R2 and R3 solutions at $\epsilon = 0.01$, $a = 1.25$. $s = 1$ almost everywhere.

Solution at Small ϵ Limits

- Since we have the symmetry $f(x, y; a, b) = f(a - x, y; a, b)$, we get the symmetry on θ_{D1} and θ_{R3}.

$$\theta_{D1}(x, y) = \theta_{D1}(a - x, y) = \theta_{D1}(x, b - y). \tag{21}$$

$$\theta_{R3}(x, y) = -\theta_{R3}(a - x, y) = \theta_{R3}(x, b - y). \tag{22}$$

- Each solution can be determined by itself on the sub–domain $\Omega' = [0, a/2] \times [0, b/2]$, with the boundary condition,

$$\theta_{D1}(x, 0) = \theta_{R3}(x, 0) = 0, \tag{23}$$

$$\theta_{D1}(0, y) = \theta_{R3}(0, y) = \pi/2, \tag{24}$$

$$\theta_{R3}(a/2, y) = 0. \tag{25}$$

So the R3 solution is restricted in a smaller space than the one of D1 solution, so the energy of R3 solution is higher than the energy of D1 solution.

Motivation

- What is happening for intermediate ϵ?
- In square case, we have bifurcation on solutions with respect to ϵ [Robinson et al., 2017].
- We work on the rectangular domains.
- The solutions R2 and R3 no longer have degenerate energies.

Motivation

- What is happening for intermediate ϵ?
- In square case, we have bifurcation on solutions with respect to ϵ [Robinson et al., 2017].
- We work on the rectangular domains.
- The solutions R2 and R3 no longer have degenerate energies.

Bifurcation Diagram [Robinson et al., 2017]

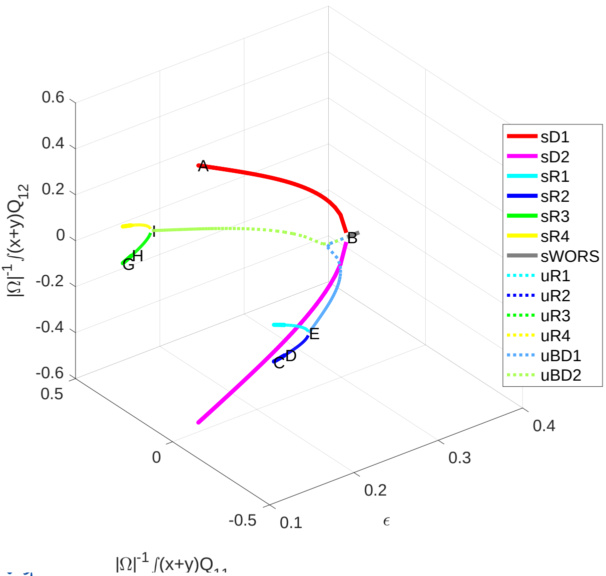

Bifurcation Problem

- We focus on the critical points of a system $F(x, y) = 0 \in \mathbb{R}^d$, where $x \in \mathbb{R}^d$ is the degree of freedoms and y is the scalar parameter. The problem is to catch the change of the solution x with respect to the parameter y.
- In our problem, we are solving $\delta I_{\mathrm{LdG}}(\mathbf{Q}, \epsilon) / \delta \mathbf{Q} = 0$ for different ϵ.
- Newton–Raphson method fails when the Hessian of energy functional has zero eigenvalues,

$$\mathrm{d}x = \left(\frac{\partial F(x, y)}{\partial x}\right)^{-1} \frac{\partial F(x, y)}{\partial y} \mathrm{d}y. \tag{26}$$

Bifurcation Problem

- We focus on the critical points of a system $F(x, y) = 0 \in \mathbb{R}^d$, where $x \in \mathbb{R}^d$ is the degree of freedoms and y is the scalar parameter. The problem is to catch the change of the solution x with respect to the parameter y.
- In our problem, we are solving $\delta I_{\mathrm{LdG}}(\mathbf{Q}, \epsilon) / \delta \mathbf{Q} = 0$ for different ϵ.
- Newton–Raphson method fails when the Hessian of energy functional has zero eigenvalues,

$$\mathrm{d}x = \left(\frac{\partial F(x, y)}{\partial x}\right)^{-1} \frac{\partial F(x, y)}{\partial y} \mathrm{d}y. \tag{26}$$

Arc–length Method

- The idea of arc–length method [Kelley, 2018] is to use the arc–length s as a new parameter, and solve a one–dimensional larger system,

$$G(x,y) = \begin{pmatrix} F(x,y) \\ N(x,y) \end{pmatrix} = \begin{pmatrix} 0 \\ 0 \end{pmatrix} \tag{27}$$

for both x and y with respect to s. Here s is the arc–length since we use the arc–length normalization equation,

$$N(x,y) = \left|\frac{\partial x}{\partial s}\right|^2 + \left(\frac{\partial y}{\partial s}\right)^2 - 1. \tag{28}$$

It is proved that if the parameter is changed from y to s, then the singularity has been eliminated and the path of solutions is homeomorphic to a line segment [Kelley, 2018].

Numerical Implementation

- We use the dimensionless Landau–de Gennes free energy.

$$\int_{\tilde{\Omega}} \left(|\nabla Q_{11}|^2 + |\nabla Q_{12}|^2 + \frac{1}{\epsilon^2} \left(Q_{11}^2 + Q_{12}^2 - 1 \right)^2 \right). \tag{29}$$

- $L_{\mathrm{el}} = 1$, $\tilde{\Omega} = [0, a] \times [0, b]$, $a \in \{1, 1.25, 1.5\}$, $b = 1$.
- Strong anchoring Dirichlet boundary condition $(Q_{11}, Q_{12}) = g_{0.3}$ on $\partial\tilde{\Omega}$.
- Finite difference method on uniform mesh with $h = 1/64$.
- Use the arc–length method to solve $G\left(Q, \epsilon^{-2}\right) = 0$. We choose the starting point at $\epsilon = 0.13$, and uniform arc–length spacing $\Delta s = 0.5$ for 100 arc–length iterations when increasing ϵ.
- Numerically study relationship between ϵ and energy and relationship among ϵ, $\fint_{\tilde{\Omega}} (x + y)\, Q_{11}$ and $\fint_{\tilde{\Omega}} (x + y)\, Q_{12}$.

Notations

- Diagonal solutions (D1, D2), rotated solutions (R1, R2, R3, R4). We can easily distinguish them by the defect strength at the corners.
- Boundary distortion (BD) solutions, $Q_{12} \equiv 0$, which have line defects in 2D, similar to WORS.
- BD1: vertical directors in the center, horizontal directors near the top and the bottom. BD2: horizontal directors in the center, vertical directors near the left and the right.
- 's': numerically stable, 'u': numerically unstable.

Example: $\Omega = [0,1] \times [0,1]$, Energy

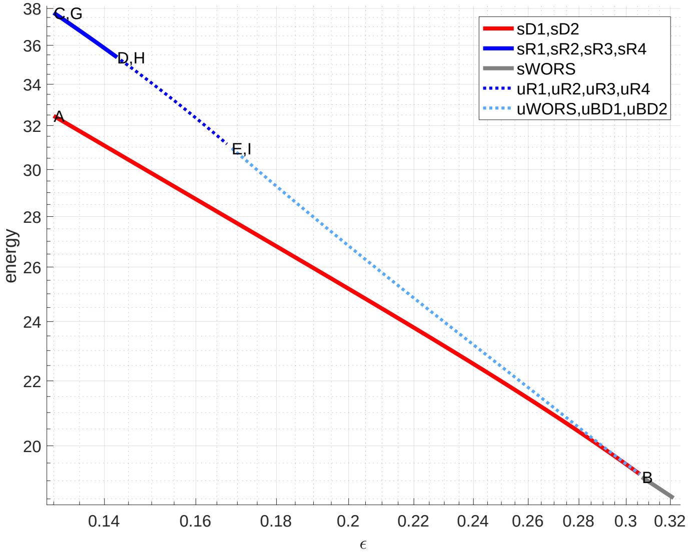

Example: $\Omega = [0, 1.25] \times [0, 1]$, Energy

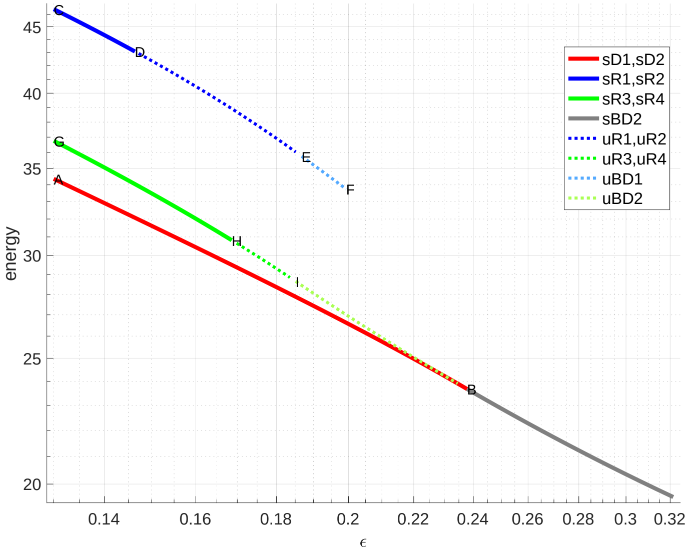

Example: $\Omega = [0, 1.5] \times [0, 1]$, Energy

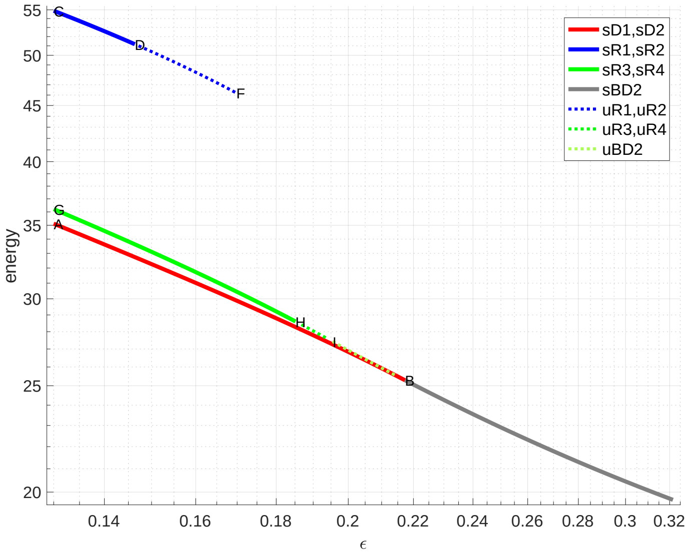

Solutions sD1 $\to$ sBD2 (A $\to$ B)

$a = 1$

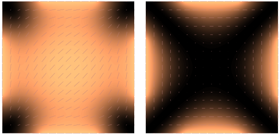

$a = 1.25$

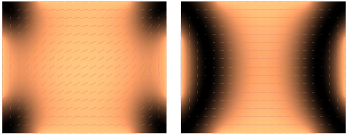

$a = 1.5$

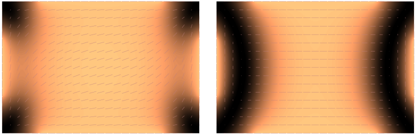

Solutions sR3 → uR3 → uBD2 → sBD2 (G → H → I → B)

$a = 1$

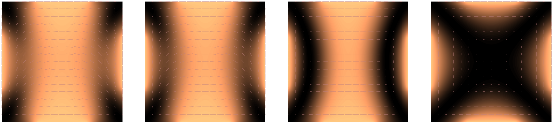

$a = 1.25$

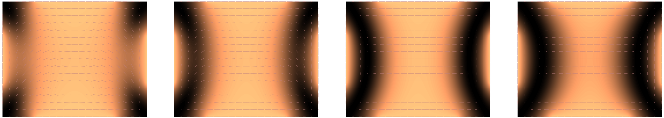

$a = 1.5$

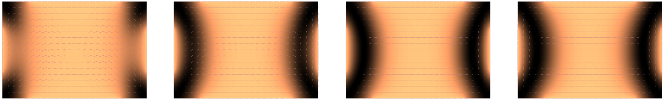

Solutions sR2 $\rightarrow$ uR2 $\rightarrow$ uBD1 $\rightarrow$ end (C $\rightarrow$ D $\rightarrow$ E $\rightarrow$ F)

$a = 1.25$, sR2 $\rightarrow$ uR2 $\rightarrow$ uBD1 $\rightarrow$ end (C $\rightarrow$ D $\rightarrow$ E $\rightarrow$ F)

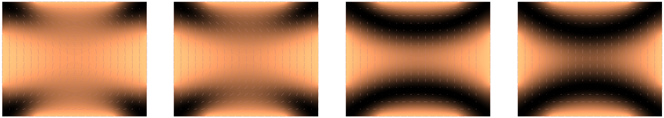

$a = 1.5$, sR2 $\rightarrow$ uR2 $\rightarrow$ end (C $\rightarrow$ D $\rightarrow$ F)

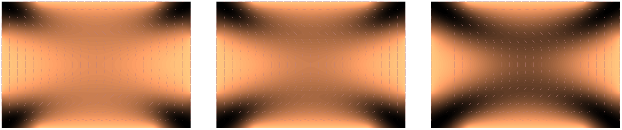

$a = 3$, sR2 $\rightarrow$ end (C $\rightarrow$ F)

Q–tensor Plot

- Try to plot a bifurcation diagram that can distinguish all eight classes of solutions (D1, D2, R1, R2, R3, R4, BD1, BD2).
- The values $\fint_{\tilde{\Omega}} Q_{11}(x, y)\,\mathrm{d}x\mathrm{d}y$ and $\fint_{\tilde{\Omega}} Q_{12}(x, y)\,\mathrm{d}x\mathrm{d}y$ can not distinguish R1–R2 pair and R3–R4 pair.
- We plot the values $\fint_{\tilde{\Omega}} (x+y)\, Q_{11}(x, y)\,\mathrm{d}x\mathrm{d}y$ and $\fint_{\tilde{\Omega}} (x+y)\, Q_{12}(x, y)\,\mathrm{d}x\mathrm{d}y$ with respect to ϵ. [Robinson et al., 2017]

Q–tensor Plot

- Try to plot a bifurcation diagram that can distinguish all eight classes of solutions (D1, D2, R1, R2, R3, R4, BD1, BD2).
- The values $\fint_{\tilde{\Omega}} Q_{11}\left(x,y\right)\mathrm{d}x\mathrm{d}y$ and $\fint_{\tilde{\Omega}} Q_{12}\left(x,y\right)\mathrm{d}x\mathrm{d}y$ can not distinguish R1–R2 pair and R3–R4 pair.
- We plot the values $\fint_{\tilde{\Omega}} \left(x+y\right) Q_{11}\left(x,y\right)\mathrm{d}x\mathrm{d}y$ and $\fint_{\tilde{\Omega}} \left(x+y\right) Q_{12}\left(x,y\right)\mathrm{d}x\mathrm{d}y$ with respect to ϵ. [Robinson et al., 2017]

Example: $\Omega = [0,1] \times [0,1]$, Q [Robinson et al., 2017]

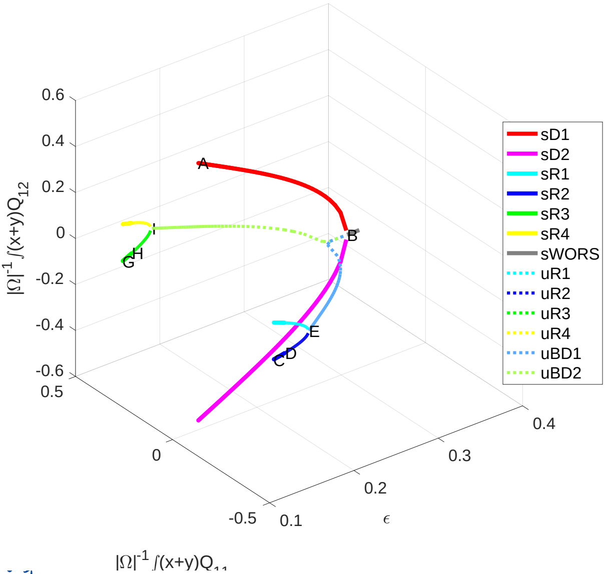

Example: $\Omega = [0,1] \times [0,1]$, Q [Robinson et al., 2017]

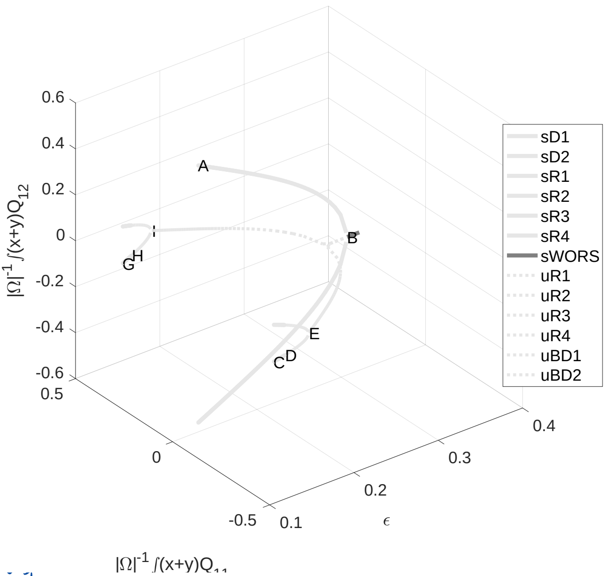

Example: $\Omega = [0,1] \times [0,1]$, Q [Robinson et al., 2017]

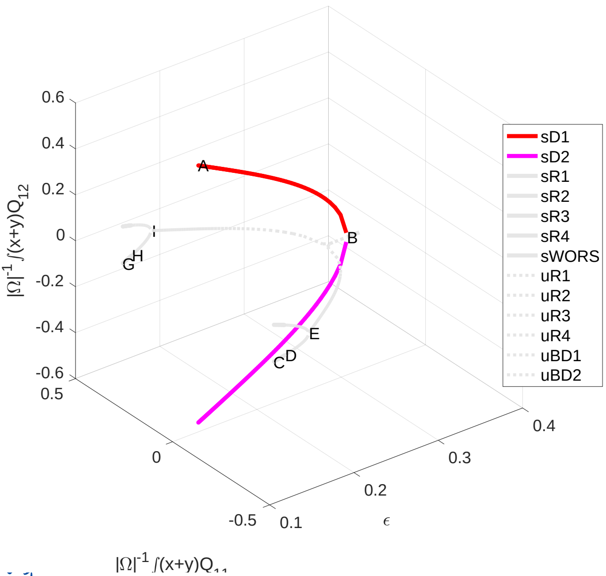

Example: $\Omega = [0,1] \times [0,1]$, Q [Robinson et al., 2017]

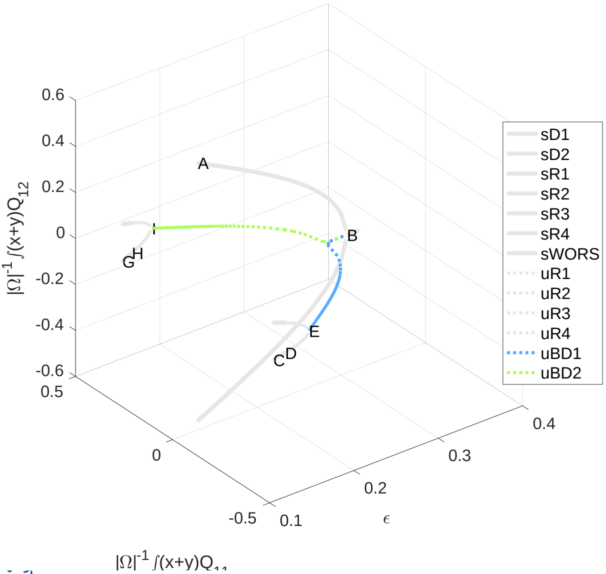

Example: $\Omega = [0,1] \times [0,1]$, Q [Robinson et al., 2017]

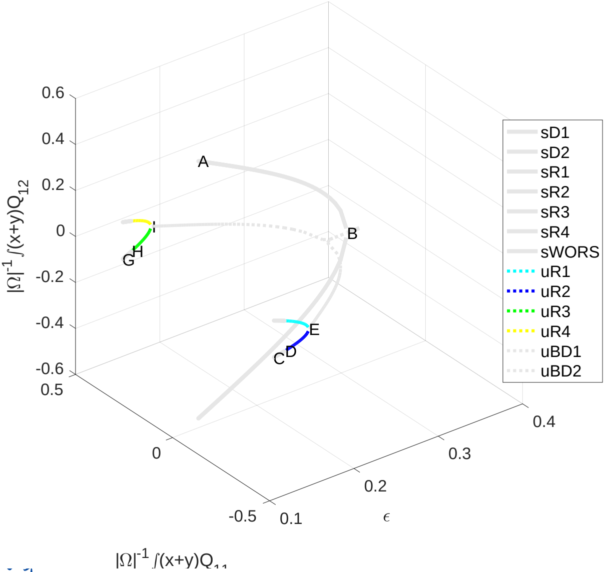

Example: $\Omega = [0,1] \times [0,1]$, Q [Robinson et al., 2017]

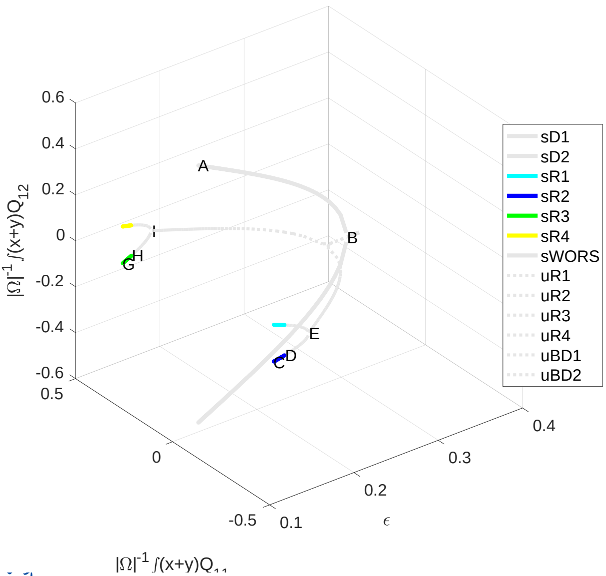

Example: $\Omega = [0, 1.25] \times [0, 1]$, Q

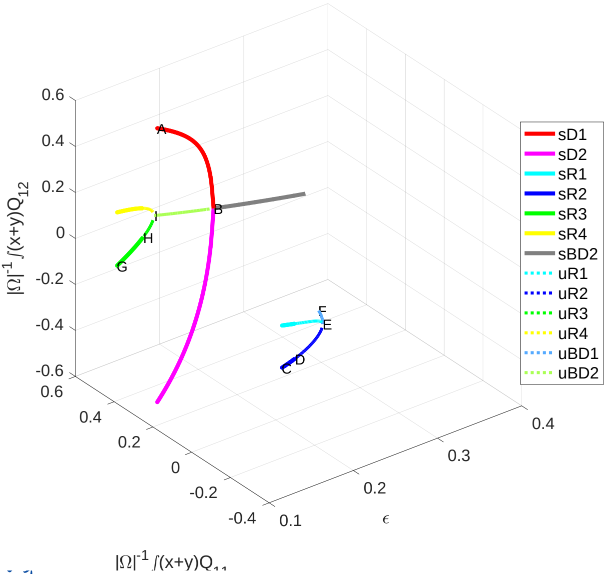

Example: $\Omega = [0,1] \times [0,1]$, Q [Robinson et al., 2017]

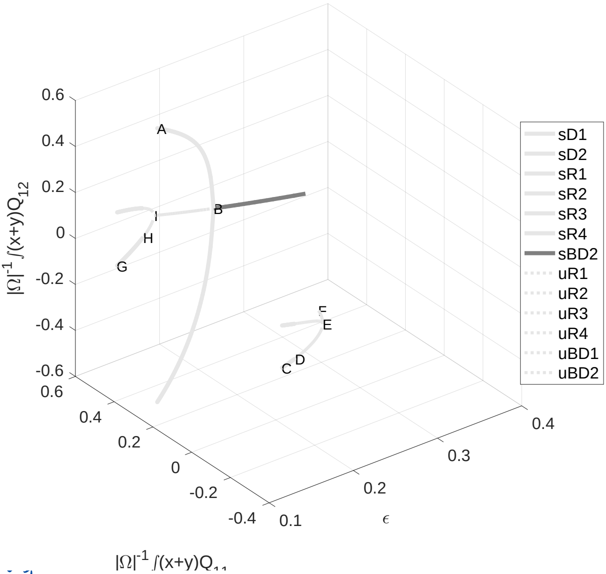

Example: $\Omega = [0,1] \times [0,1]$, Q [Robinson et al., 2017]

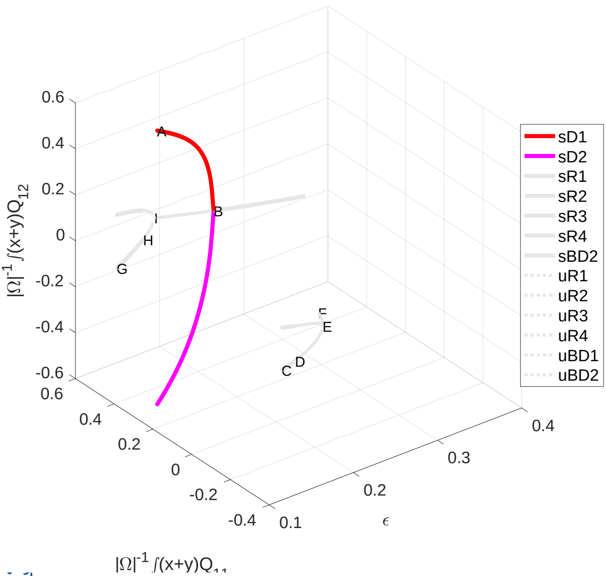

Example: $\Omega = [0,1] \times [0,1]$, Q [Robinson et al., 2017]

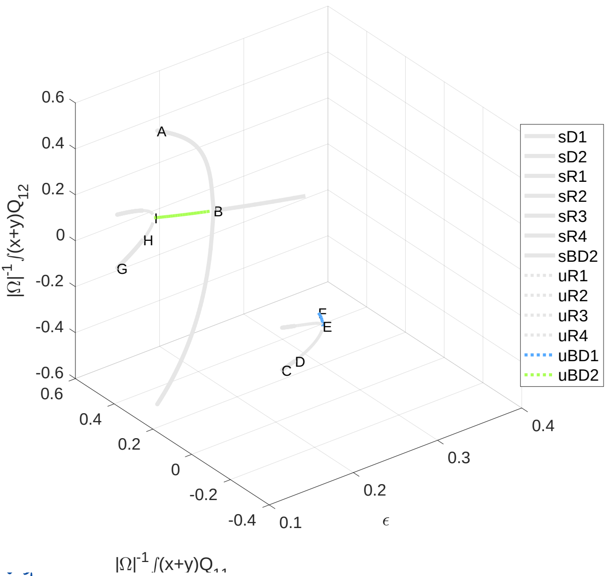

Example: $\Omega = [0,1] \times [0,1]$, Q [Robinson et al., 2017]

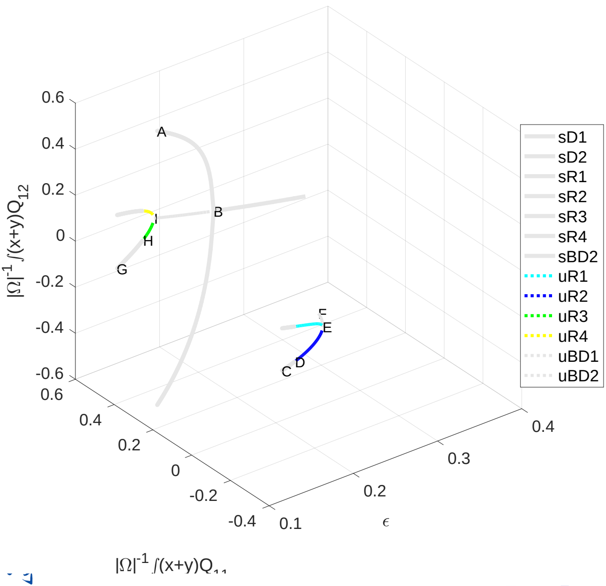

Example: $\Omega = [0,1] \times [0,1]$, Q [Robinson et al., 2017]

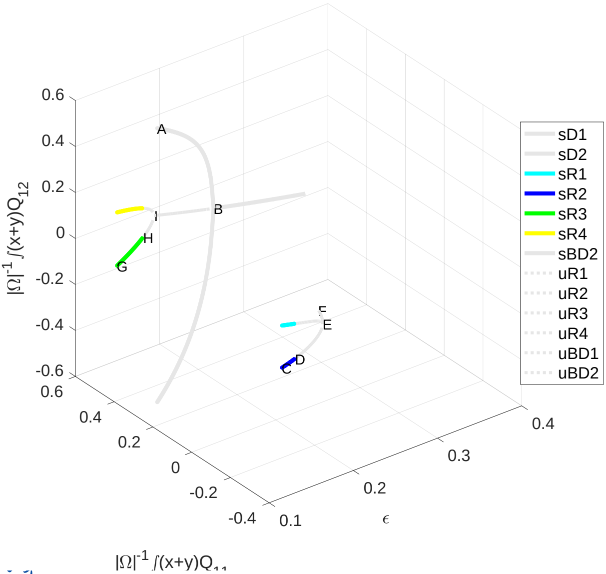

Example: $\Omega = [0, 1.5] \times [0, 1]$, Q

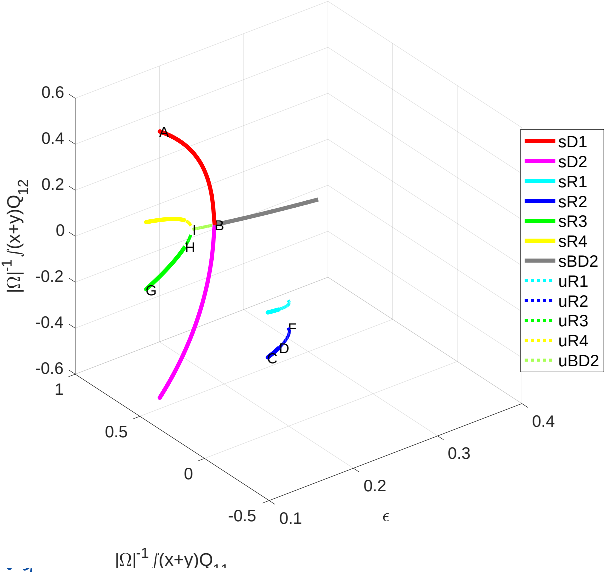

Example: $\Omega = [0,1] \times [0,1]$, Q [Robinson et al., 2017]

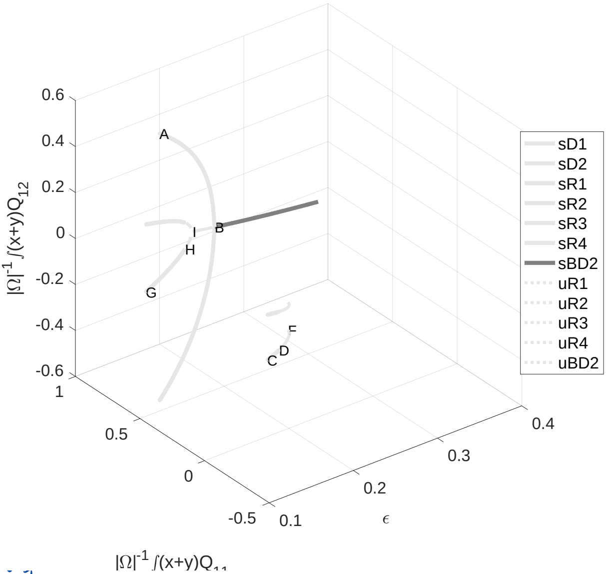

Example: $\Omega = [0,1] \times [0,1]$, Q [Robinson et al., 2017]

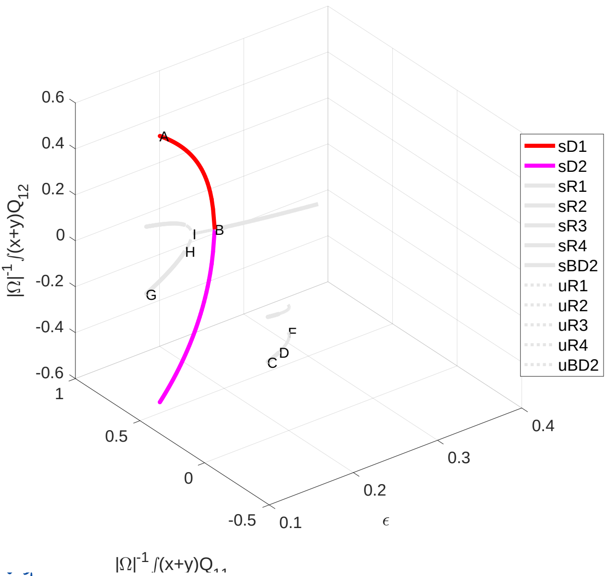

Example: $\Omega = [0,1] \times [0,1]$, Q [Robinson et al., 2017]

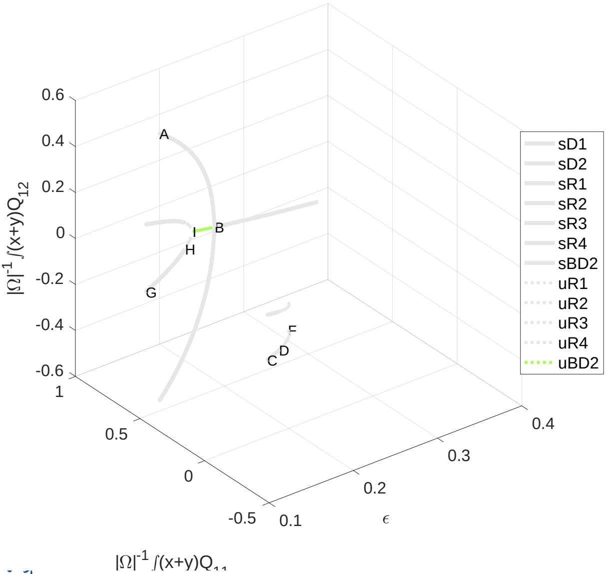

Example: $\Omega = [0,1] \times [0,1]$, Q [Robinson et al., 2017]

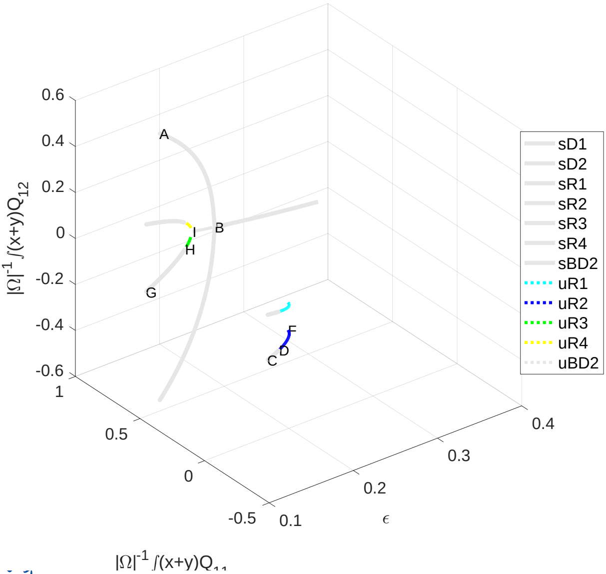

Example: $\Omega = [0,1] \times [0,1]$, Q [Robinson et al., 2017]

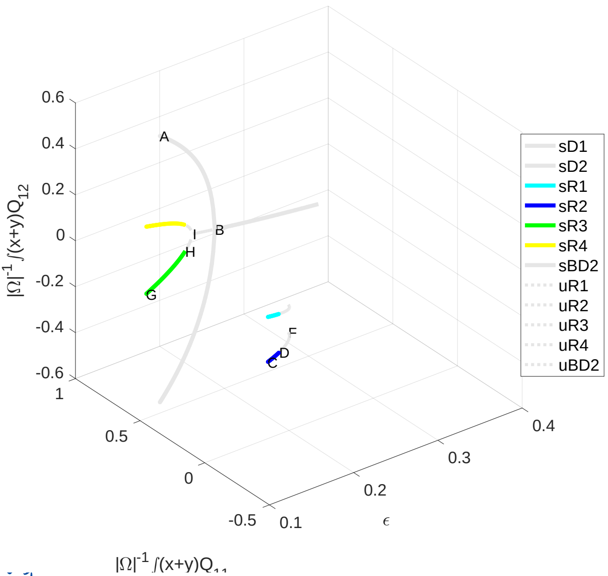

LdG Bifurcation Diagram for Rectangular Domains

- One connected component at $a = 1$. Square case [Robinson et al., 2017].
- Two connected components at $a = 1.25$. sBD1 disappears.
- Three connected components at $a = 1.5$. sBD1 and uBD1 disappear.
- Three connected components at larger a. sBD1, uBD1, uR1 and uR2 disappear.
- When increasing a from 1, the solutions R1, R2 and BD1 are hard to survive due to the high energy from the serious distortion.

LdG Bifurcation Diagram for Rectangular Domains

- One connected component at $a = 1$. Square case [Robinson et al., 2017].
- Two connected components at $a = 1.25$. sBD1 disappears.
- Three connected components at $a = 1.5$. sBD1 and uBD1 disappear.
- Three connected components at larger a. sBD1, uBD1, uR1 and uR2 disappear.
- When increasing a from 1, the solutions R1, R2 and BD1 are hard to survive due to the high energy from the serious distortion.

LdG Bifurcation Diagram for Rectangular Domains

- One connected component at $a = 1$. Square case [Robinson et al., 2017].
- Two connected components at $a = 1.25$. sBD1 disappears.
- Three connected components at $a = 1.5$. sBD1 and uBD1 disappear.
- Three connected components at larger a. sBD1, uBD1, uR1 and uR2 disappear.
- When increasing a from 1, the solutions R1, R2 and BD1 are hard to survive due to the high energy from the serious distortion.

Conclusion

- LdG solutions on 2D rectangular domains with tangential boundary condition.
- Large ϵ limit, $\Delta Q_{11} = 0$.
- Small ϵ limit, $\Delta\theta = 0$.
- Intermediate ϵ, bifurcation depends on a.

Conclusion

- LdG solutions on 2D rectangular domains with tangential boundary condition.
- Large ϵ limit, $\Delta Q_{11} = 0$.
- Small ϵ limit, $\Delta\theta = 0$.
- Intermediate ϵ, bifurcation depends on a.

Thank you!

Any Question?

Reference I

Bethuel, F., Brezis, H., and Hélein, F. (1993).
Asymptotics for the minimization of a ginzburg-landau functional.
Calculus of Variations and Partial Differential Equations, 1(2):123–148.

de Gennes, P. G. and Prost, J. (1995).
The physics of liquid crystals.
Number 83. Oxford university press.

Henao, D., Majumdar, A., and Pisante, A. (2017).
Uniaxial versus biaxial character of nematic equilibria in three dimensions.
Calculus of Variations and Partial Differential Equations, 56(2):55.

Reference II

Kelley, C. T. (2018).
Numerical methods for nonlinear equations.
Acta Numerica, 27:207287.

Luo, C., Majumdar, A., and Erban, R. (2012).
Multistability in planar liquid crystal wells.
Physical Review E, 85(6):061702.

Majumdar, A. and Zarnescu, A. (2010).
Landau–de gennes theory of nematic liquid crystals: the oseen–frank limit and beyond.
Archive for rational mechanics and analysis, 196(1):227–280.

Mottram, N. J. and Newton, C. J. (2014).
Introduction to q-tensor theory.
arXiv preprint arXiv:1409.3542.

Reference III

Robinson, M., Luo, C., Farrell, P. E., Erban, R., and Majumdar, A. (2017).
From molecular to continuum modelling of bistable liquid crystal devices.
Liquid Crystals, 44(14-15):2267–2284.

Tsakonas, C., Davidson, A., Brown, C., and Mottram, N. (2007).
Multistable alignment states in nematic liquid crystal filled wells.
Applied physics letters, 90(11):111913.